Mathematical Modeling of Longitudinal Compressive Failure in Fiber Reinforced Composites as Shear Banding DUE to Strain Localization

Takeaki Nadabe
Department of Advanced Energy, Graduate School of Frontier Sciences,
the University of Tokyo, Kashiwa, Chiba, Japan
E-mail: nadabe@smart.k.u-tokyo.ac.jp

Abstract—*This study investigates the mathematical modeling of longitudinal compressive failure in fiber reinforced composites as shear banding due to strain localization. Firstly the numerical simulation of longitudinal compressive failure is conducted. The simulated results show that at one moment of the loading, the localized deformation catastrophically appears in the material, and in this initiation of the localized deformation, the reduction of tangent shear stiffness plays an important role. Then a set of mathematical equations is obtained for the deformation of composite materials, and the mathematical solution of the equations is considered. There exists a state where arbitrariness appears in the solution of equations expressing deformation of composite materials, and it is indicated that the onset of arbitrariness in solution of equations expressing deformation of composite materials is closely related with the initiation of longitudinal compressive failure, and also related with the initiation of narrow localized band in the materials.*

Keywords: *Mathematical Modeling, Longitudinal Compressive Failure, Strength Analysis, Composite Materials*

INTRODUCTION

Composite materials commonly have complex internal structures including fibers, matrix, interfaces and interlaminar regions, and when precise evaluation of fracture strength of the material is conducted, the internal fracture process in the materials is necessary to be taken into account in the numerical analysis. In recent years, composite materials are being increasingly used in several industrial fields, and the precise evaluation of mechanical response of the material under various loading condition and environmental condition increases the necessity in design and improvement of industrial products [1–3]. Compressive failure is one of the typical failure modes in fiber reinforced composite materials, and fracture strength in compressive failure often becomes one of the limiting factors at the design phase of structural elements [2–3]. This study investigates the mathematical modeling of longitudinal compressive failure in fiber reinforced composite materials. The purpose of this study is to establish the numerical analysis method to predict the mechanical response of composite materials which changes under different loading condition and environmental condition.

NUMERICAL SIMULATION OF LONGITUDI-NAL COMPRESSIVE FAILURE

Numerical Model

Firstly the numerical simulation of longitudinal compressive failure is conducted. Finite element method is used to simulate the longitudinal compressive failure. Fig. 1 shows the numerical model of this analysis. The white and gray elements in Fig. 1 represent fibers and matrix, respectively. Each fiber and matrix is modeled by two-dimensional plate elements. The elements have eight nodes and four integration points in order to avoid the shear locking and zero-energy mode deformation particularly in plas-tic deformation. The one fiber placed at the center has the initial misalignment as shown in Fig. 1. In this analysis, carbon fiber/ epoxy resin AS4/3501-6 is assumed as the material, and the material property values shown in Ref. [5] are applied.

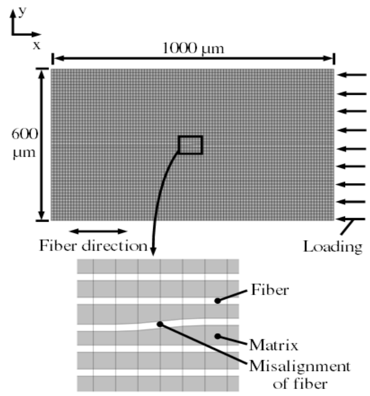

Fig. 1: Numerical Model of Composite Material

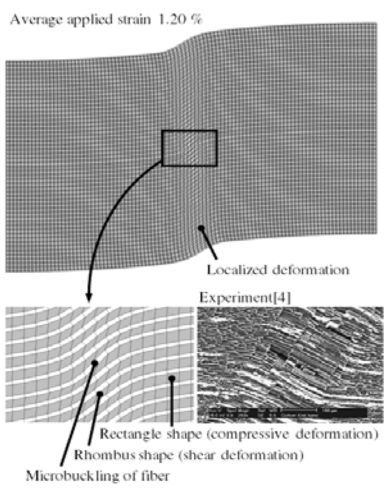

Fig. 2: Simulated Results of Deformation

Simulated Results and Discussion

Figure 2 shows the simulated results of deformation of the material. Simulated results show that in the initial state of the loading, the stress concentration occurs in the material around the initial misalignment of fiber, and when the applied load is increased, local areas of matrix around the stress concentration start to yield, and deformation is locally increased. At one moment of the loading, a large deformation occurs within a narrow band, and a band of localized deformation develops rapidly. This band of localized deformation passes across the misalignment part of center fiber. As shown in Fig. 2, fibers cause bending deformation, and fiber direction is largely rotated. Matrix causes shear deformation, and the shape of the elements is close to rhombus shape which is rectangle shape in initial state. After the yielding of matrix, the elastic-plastic tangent shear stiffness of matrix significantly reduces, and the shear strain rapidly increases. Then the shear deformation of this part of matrix increases, and due to the shear deformation of the part, the band of localized deformation is formed. The reduction of shear stiffness of matrix is the essential factor in the initiation of the localized deformation of the material.

MATHEMATICAL MODELING OF LONGITUDI-NAL COMPRESSIVE FAILURE

Equations Expressing Deformation of Composite Materials

Here, the equations expressing deformation of composite materials are compiled. The equations consist of motion equation and constitutive equation. The motion equation is represented as the following:

$$\rho_0 \frac{\partial^2 u_i}{\partial t^2} = \frac{\partial P_{ij}}{\partial X_j} + \rho_0 f_i \tag{1}$$

where ρ_0 is density, t is time, u_i is displacement, X_j is coordinate at reference configuration, P_{ij} is the first Piola-Kirchhoff stress and f_i is external force. The nonlinear stress-strain relation of composite materials is represented by the nonlinear deformation theory shown by Tohgo *et al.* [6].

$$\begin{aligned} d\boldsymbol{\sigma} &= \boldsymbol{C}_{comp} d\boldsymbol{\varepsilon} \\ \boldsymbol{C}_{comp} &= \boldsymbol{C}_m \left\{ (1-V_f)(\boldsymbol{C}_f - \boldsymbol{C}_m)\boldsymbol{S} + \boldsymbol{C}_m \right\}^{-1} \boldsymbol{K} \\ \boldsymbol{K} &= (1-V_f)\left\{ (\boldsymbol{C}_f - \boldsymbol{C}_m)\boldsymbol{S} + \boldsymbol{C}_m \right\} + V_f \boldsymbol{C}_f \end{aligned} \tag{2}$$

where $d\boldsymbol{\sigma}$ is stress rate, $d\boldsymbol{\varepsilon}$ is strain rate, $\boldsymbol{C}_{comp}$, $\boldsymbol{C}_f$ and $\boldsymbol{C}_m$ are constitutive tensors of composites, fibers and matrix, respectively, V_f is fiber volume fraction and $\boldsymbol{S}$ is Eshelby tensor. In order to apply the stress-strain relation in Eq. (2) in numerical analysis, evaluation of equivalent stress of matrix is necessary. The following relation is applied to evaluate the equivalent stress of matrix from the applied stress in composite materials:

$$d\boldsymbol{\sigma}_m = \boldsymbol{C}_m (\boldsymbol{S}-\boldsymbol{I}) \boldsymbol{K}^{-1} \left\{ \boldsymbol{C}_m + (\boldsymbol{C}_f - \boldsymbol{C}_m)\boldsymbol{S} \right\} (\boldsymbol{S}-\boldsymbol{I})^{-1} \boldsymbol{C}_m^{-1} d\boldsymbol{\sigma} \tag{3}$$

where $d\boldsymbol{\sigma}_m$ is stress rate of matrix and $\boldsymbol{I}$ is unit tensor. Then the effect of geometrical nonlinearity during the material deformation is considered. Here the constitutive tensor in spacial description is defined in the relation between the second Piola-Kirchhoff stress and the right Cauchy-Green deformation tensor:

$$C_{abcd}^{spa} = \frac{\partial S_{ab}}{\partial C_{cd}^{CG}} \tag{4}$$

where C_{abcd}^{spa} is constitutive tensor in spacial description, S_{ab} is the second Piola-Kirchhoff stress and C_{cd}^{CG} is the right Cauchy-Green deformation tensor. The constitutive tensor in material description is represented by the constitutive tensor in spacial description as follows:

$$\begin{aligned} C_{ijkl}^{mat} &= 2J^{-1} F_{ia} F_{jb} F_{kc} F_{ld} C_{abcd}^{spa} \\ &= 2 \frac{1}{J} \frac{\partial x_i}{\partial X_a} \frac{\partial x_j}{\partial X_b} \frac{\partial x_k}{\partial X_c} \frac{\partial x_l}{\partial X_d} C_{abcd}^{spa} \end{aligned} \tag{5}$$

where C_{ijkl}^{mat} is constitutive tensor in material description, F_{ia} is deformation gradient, $J = \det F_{ij}$ is Jacobian and x_i is coordinate at present configuration. Cauchy stress is represented by the second Piola-Kirchhoff stress, deformation gradient and Jacobian as follows:

$$\sigma_{ij} = J^{-1} F_{ik} S_{kl} F_{jl} \tag{6}$$

$$\begin{aligned} \dot{\sigma}_{ij} &= J^{-1} \dot{F}_{ik} S_{kl} F_{jl} + J^{-1} F_{ik} \dot{S}_{kl} F_{jl} \\ &+ J^{-1} F_{ik} S_{kl} \dot{F}_{jl} - \dot{J} J^{-1} F_{ik} S_{kl} F_{jl} \end{aligned} \tag{7}$$

where σ_{ij} is Cauchy stress and $\dot{\sigma}_{ij}$ is the material time derivative of Cauchy stress. Here, the time derivative of deformation gradient and Jacobian is:

$$\dot{F}_{ij} = L_{ik} F_{kj}, \; \dot{J} = L_{ii} \tag{8}$$

where L_{ik} is velocity gradient. Then

$$\dot{\sigma}_{ij} = J^{-1} L_{im} F_{mk} S_{kl} F_{jl} + J^{-1} F_{ik} \dot{S}_{kl} F_{jl}$$

$$+J^{-1}F_{ik}S_{kl}F_{ml}L_{jm} - J^{-1}L_{mm}F_{ik}S_{kl}F_{jl}$$

$$= J^{-1}F_{ik}\dot{S}_{kl}F_{jl} + L_{ik}\sigma_{kj} + \sigma_{ik}L_{jk} - \sigma_{ij}L_{ll} \tag{9}$$

Where:

$$\dot{S}_{kl} = C^{spa}_{klmn} \cdot \dot{C}^{CG}_{mn} = C^{spa}_{klmn}\dot{F}_{om}F_{on} + C^{spa}_{klmn}F_{om}\dot{F}_{on}$$

$$= C^{spa}_{klmn}L_{op}F_{pm}F_{on} + C^{spa}_{klmn}F_{om}L_{op}F_{pn} \tag{10}$$

$$J^{-1}F_{ik}\dot{S}_{kl}F_{jl} = J^{-1}F_{ik}F_{jl}F_{pm}F_{on}C^{spa}_{klmn}L_{op}$$

$$+J^{-1}F_{ik}F_{jl}F_{om}F_{pn}C^{spa}_{klmn}L_{op}$$

$$= \frac{1}{2}C^{mat}_{ijpo}L_{op} + \frac{1}{2}C^{mat}_{ijop}L_{op}$$

$$= C^{mat}_{ijkl} \cdot \frac{1}{2}\left(L_{lk} + L_{kl}\right) = C^{mat}_{ijkl}D_{kl} \tag{11}$$

Therefore:

$$\dot{\sigma}_{ij} = C^{mat}_{ijkl}D_{kl} + L_{ik}\sigma_{kj} + \sigma_{ik}L_{jk} - \sigma_{ij}L_{ll} \tag{12}$$

This coincides with the formulation of Truesdell rate of Cauchy stress. Therefore, here the formulation of finite deformation is based on Truesdell rate of Cauchy stress. Then the rate of the first Piola-Kirchhoff stress is represented as follows:

$$\dot{P}_{ij} = J\frac{\partial X_j}{\partial x_k}\left(\dot{\sigma}_{ik} + \sigma_{ik}L_{ll} - \sigma_{il}L_{kl}\right)$$

$$= J\frac{\partial X_j}{\partial x_m}\left(C^{mat}_{imkl}D_{kl} + \sigma_{lm}L_{il}\right)$$

$$= J\frac{\partial X_j}{\partial x_m}\left(C^{mat}_{imkl} + \sigma_{lm}\delta_{ik}\right)\frac{\partial \dot{u}_k}{\partial x_l} \tag{13}$$

where δ_{ik} is Kronecker delta. From Eqs. (1) and (13), a set of equations expressing deformation of composite materials is obtained:

$$\rho_0\frac{\partial^2 u_i}{\partial t^2} = \frac{\partial P_{ij}}{\partial X_j} + \rho_0 f_i \tag{14}$$

$$\dot{P}_{ij} = J\frac{\partial X_j}{\partial x_m}\left(C^{mat}_{imkl} + \sigma_{lm}\delta_{ik}\right)\frac{\partial \dot{u}_k}{\partial x_l} \tag{15}$$

Arbitrariness Appearing in Solution of Equ-ations in Deformation of Composite Materials

Equations (14) and (15) are unified to one differential equation:

$$\rho_0\frac{\partial^2 \dot{u}_i}{\partial t^2} - \rho_0\dot{f}_i = \frac{\partial}{\partial X_j}\left(A_{ijkl}\frac{\partial \dot{u}_k}{\partial x_l}\right) \tag{16}$$

where tensor A_{ijkl} is

$$A_{ijkl} = J\frac{\partial X_j}{\partial x_m}\left(C^{mat}_{imkl} + \sigma_{lm}\delta_{ik}\right) \tag{17}$$

Equation (16) plays a role of governing equation in the deformation of composite materials. When the reference configuration is taken at the moment of the present time, and in the place where the external force doesn't act, Eq. (16) becomes as follows:

$$\rho\frac{\partial^2 \dot{u}_i}{\partial t^2} = \frac{\partial}{\partial x_j}\left(A_{ijkl}\frac{\partial \dot{u}_k}{\partial x_l}\right) \tag{18}$$

where ρ is density at the present time. Here, we conduct the transformation of coordinate system for this equation. Firstly each variable is transformed as the following in the transformation of coordinate system.

$$dx_i = \frac{\partial x_i}{\partial x'_a}dx'_a,\ \dot{u}_i = \frac{\partial x_i}{\partial x'_a}\dot{u}'_a,\ \frac{\partial}{\partial x_l} = \frac{\partial x'_d}{\partial x_l}\frac{\partial}{\partial x'_d}$$

$$L_{kl} = \frac{\partial x_k}{\partial x'_c}\frac{\partial x'_d}{\partial x_l}\frac{\partial u'_c}{\partial x'_d} = \frac{\partial x_k}{\partial x'_c}\frac{\partial x'_d}{\partial x_l}L'_{cd},\ \sigma_{ij} = \frac{\partial x_i}{\partial x'_a}\frac{\partial x_j}{\partial x'_b}\sigma'_{ab}$$

$$A_{ijkl} = \frac{\partial x_i}{\partial x'_a}\frac{\partial x_j}{\partial x'_b}\frac{\partial x'_c}{\partial x_k}\frac{\partial x_l}{\partial x'_d}A'_{abcd} \tag{19}$$

where x'_a is the coordinate system after the transformation. Then Eq. (18) is transformed as follows:

$$\rho\frac{\partial^2 \dot{u}'_a}{\partial t^2} = \frac{\partial}{\partial x'_b}\left(A'_{abcd}\frac{\partial \dot{u}'_c}{\partial x'_d}\right) \tag{20}$$

Commonly the governing equations for natural phenomena do not change their form in the coordinate transformation. Then, when the deformation is locally independent to 2' and 3' directions, $\partial/\partial x'_2$ and $\partial/\partial x'_3$ are equal to zero, and when the deformation is quasi-static, $\partial/\partial t$ becomes equal to zero, which corresponds with the case when inertia term is infinitesimal, then Eq. (20) becomes as follows:

$$\frac{\partial}{\partial x'_1}\left(A'_{a1c1}\frac{\partial \dot{u}'_c}{\partial x'_1}\right) = 0 \tag{21}$$

Here, the eigenvalue problem of the tensor A'_{a1c1} is considered. Using the eigenvalue λ' and the eigenvector v'_c of the tensor A'_{a1c1}, the eigenvalue problem is represented as:

$$A'_{a1c1}v'_c = \lambda' v'_c \quad (22)$$

When the tensor A'_{a1c1} has zero eigenvalues, Eq. (22) becomes as follows:

$$A'_{a1c1}v'_c = 0 \quad (23)$$

Multiplying the arbitrary function $\phi'(x'_1)$:

$$A'_{a1c1}v'_c\phi'(x'_1) = 0 \quad (24)$$

Then taking the partial differenciation of x'_1:

$$A'_{a1c1}v'_c\frac{\partial}{\partial x'_1}\phi'(x'_1) = 0 \quad (25)$$

This equation means that $\dot{u}'_c = v'_c\phi'(x'_1)$ is one of the solution of Eq. (21). Since $\dot{u}'_c = v'_c\phi'(x'_1)$ is the solution of Eq. (21) for arbitrary function $\phi'(x'_1)$, Eq. (21) have multiple solutions, or the arbitrariness appears in the solution of Eq. (21). This case causes when the tensor A'_{a1c1} has zero eigenvalues. When the tensor A'_{a1c1} has zero eigenvalues, the determinant of A'_{a1c1} becomes zero:

$$\det(A'_{a1c1}) = 0 \quad (26)$$

From Eq. (19), the tensor A'_{a1c1} is represented by the original coordinate system of tensor A_{ijkl}:

$$A'_{a1c1} = A_{ijkl}\frac{\partial x'_a}{\partial x_i}\frac{\partial x'_1}{\partial x_j}\frac{\partial x_k}{\partial x'_c}\frac{\partial x'_1}{\partial x_l} \quad (27)$$

Here, we introduce two tensors n_j and J_{ai} which express the coordinate transformation:

$$n_j = \frac{\partial x'_1}{\partial x_j},\; J_{ai} = \frac{\partial x'_a}{\partial x_i} \quad (28)$$

Then Eq. (26) becomes as follows:

$$\det(A'_{a1c1}) = \det\left(A_{ijkl}n_jn_lJ_{ai}J_{ck}^{-1}\right)$$
$$= \det\left(A_{ijkl}n_jn_l\right)\cdot\det\left(J_{ai}\right)\cdot\det\left(J_{ck}^{-1}\right) = 0 \quad (29)$$

Since $\det(J_{ai}) \neq 0$:

$$\det\left(A_{ijkl}n_jn_l\right) = 0 \quad (30)$$

When we put the tensor $A_{ijkl}n_jn_l$ as a_{ik}, the determinant of Eq. (30) is explicitly represented in two-dimensional as the following:

$$\det a_{ik} = a_{11}a_{22} - a_{12}a_{21} = 0 \quad (31)$$

In fiber reinforced composite materials, commonly the elastic modulus in fiber axial direction has much higher value than the value of transverse direction and stress value, and because of this, C^{mat}_{1111} has much higher value than the other components of constitutive tensor C^{mat}_{ijkl} and the components of stress tensor σ_{ij}, that is $C^{mat}_{1111} >> C^{mat}_{ijkl}$, σ_{ij} $\left(C^{mat}_{ijkl} \neq C^{mat}_{1111}\right)$. Since only A_{1111} and a_{11} includes C^{mat}_{1111}, $A_{1111} >> A_{ijkl}$ $\left(A_{ijkl} \neq A_{1111}\right)$ and $a_{11} >> a_{ik}$ $\left(a_{ik} \neq a_{11}\right)$. Thus the equation becomes,

$$a_{22} = \frac{a_{12}a_{21}}{a_{11}} \approx 0 \quad (32)$$

Here the vector n_j is represented using an angle β as follows:

$$n_j = \frac{\partial x'_1}{\partial x_j} = \left(\cos\beta \quad \sin\beta\right) \quad (33)$$

Then a_{22} is represented as follows:

$$a_{22} = A_{2j2l}n_jn_l$$
$$= C^{mat}_{2j2l}n_jn_l + \sigma_{jl}n_jn_l$$
$$= \left(C^{mat}_{2121} + \sigma_{11}\right)\cos^2\beta + \left(C^{mat}_{2122} + C^{mat}_{2221} + 2\sigma_{12}\right)$$
$$\cdot\cos\beta\sin\beta + \left(C^{mat}_{2222} + \sigma_{22}\right)\sin^2\beta \approx 0 \quad (34)$$

From this equation:

$$-\sigma_{11} \approx C^{mat}_{2121} + \left(C^{mat}_{2222} + \sigma_{22}\right)\tan^2\beta$$
$$+\left(C^{mat}_{2122} + C^{mat}_{2221} + 2\sigma_{12}\right)\tan\beta \quad (35)$$

$-\sigma_{11}$ is the value of applied compressive stress to the material in longitudinal direction. When this applied stress reaches the value of right hand side of Eq. (35), the determinant of Eq. (30) becomes equal to zero, and the arbitrariness is allowed to appear, which means the instability appears in the material and microbuckling is able to occur in the actual situations. The value of $-\sigma_{11}$ at the time of being equal to right hand side of Eq. (35) is considered as the critical compressive stress σ_{cr} or the buckling stress in microbuckling:

$$\sigma_{cr} \approx C^{mat}_{2121} + \left(C^{mat}_{2222} + \sigma_{22}\right)\tan^2\beta$$
$$+\left(C^{mat}_{2122} + C^{mat}_{2221} + 2\sigma_{12}\right)\tan\beta \quad (36)$$

Using elastic-plastic tangent shear modulus G^{ep}_{LT}, transverse tangent modulus E^{ep}_T, in-plane Poisson's ratio

ν_{12} and ν_{21} and shear stress τ_{12}, the equation becomes as follows:

$$\sigma_{cr} \approx G_{LT}^{ep} + \left(\frac{1}{1-\nu_{12}\nu_{21}} E_T^{ep} + \sigma_{22} \right) \tan^2 \beta$$

$$+ \left(C_{2122}^{mat} + C_{2221}^{mat} + 2\tau_{12} \right) \tan \beta \qquad (37)$$

In the case of uniaxial compression and if C_{2122}^{mat} and C_{2221}^{mat} are close to zero, the compressive strength is approximately represented as follows,

$$\sigma_{cr} \approx G_{LT}^{ep} + \frac{1}{1-\nu_{12}\nu_{21}} E_T^{ep} \tan^2 \beta \qquad (38)$$

Equation (38) corresponds with the expression for longitudinal compressive strength of composite materials shown in Ref. [7]. It is indicated that the arbitrariness condition in equations of deformation of composite materials is closely related with the initiation condition of compressive failure in composite materials.

Moreover, the critical stress value is also represented by the constituent properties of fibers and matrix. From Eq. (2):

$$G_{LT}^{ep} \approx G_m^{ep} \cdot \frac{(1-V_f)\{(G_{fLT}^e - G_m^{ep})S_{LT} + G_m^{ep}\} + V_f G_{fLT}^e}{(1-V_f)(G_{fLT}^e - G_m^{ep})S_{LT} + G_m^{ep}}$$

$$\approx G_m^{ep} \cdot \frac{\{(1-V_f)S_{LT} + V_f\}G_{fLT}^e + (1-V_f)(1-S_{LT})G_m^{ep}}{(1-V_f)S_{LT}G_{fLT}^e + \{1-(1-V_f)S_{LT}\}G_m^{ep}} \qquad (39)$$

where G_m^{ep} is the elastic-plastic tangent shear modulus of matrix, G_{fLT}^e is the elastic in-plane shear modulus of fiber and S_{LT} is the shear component of Eshelby tensor. When the shear modulus of fiber is much higher than the shear modulus of matrix $G_{fLT}^e >> G_m^{ep}$:

$$G_{LT}^{ep} \approx G_m^{ep} \cdot \frac{\{(1-V_f)S_{LT} + V_f\}G_{fLT}^e}{(1-V_f)S_{LT}G_{fLT}^e}$$

$$\approx G_m^{ep} \cdot \left(1 + \frac{V_f}{1-V_f} S_{LT}^{-1} \right) \qquad (40)$$

The Eshelby tensor depends on the geometrical shape of reinforcement fibers. Here, two kinds of fibers shown in Fig. 3 are assumed. The case 1 in Fig. 3 is the case where fibers and matrix have plate shape, and the case 2 in Fig. 3 is the case where fibers are cylinder solids and matrix surrounds fibers. In case 1, the value of Eshelby tensor in shear component is $S_{LT} = 1$. Then:

$$G_{LT}^{ep} \approx G_m^{ep} \cdot \left(1 + \frac{V_f}{1-V_f} \right) = \frac{G_m^{ep}}{1-V_f} \qquad (41)$$

$$\sigma_{cr} \approx \frac{G_m^{ep}}{1-V_f} \qquad (42)$$

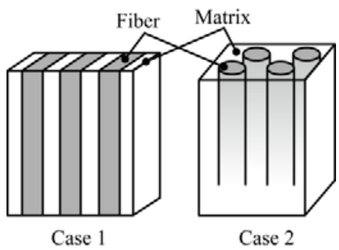

Fig. 3: Two Cases of Composite Material

On the other hand, in case 2, $S_{LT} = 1/2$. Then:

$$G_{LT}^{ep} \approx G_m^{ep} \cdot \left(1 + \frac{2V_f}{1-V_f} \right) = \frac{1+V_f}{1-V_f} G_m^{ep} \qquad (43)$$

$$\sigma_{cr} \approx \frac{1+V_f}{1-V_f} G_m^{ep} \qquad (44)$$

In addition, the elastic-plastic tangent shear modulus of matrix is closely related with the current yield state of matrix. From Eq. (3):

$$d\tau_m \approx \frac{S_{LT}G_{fLT}^e + (1-S_{LT})G_m^{ep}}{\{V_f + (1-V_f)S_{LT}\}G_{fLT}^e + (1-V_f)(1-S_{LT})G_m^{ep}} d\tau_{12,\,comp} \qquad (45)$$

where $d\tau_m$ is shear stress rate of matrix and $d\tau_{12,\,comp}$ is applied shear stress rate of composite materials. When the shear modulus of fiber is much higher than the shear modulus of matrix $G_{fLT}^e >> G_m^{ep}$:

$$d\tau_m \approx \frac{S_{LT}G_{fLT}^e}{\{V_f + (1-V_f)S_{LT}\}G_{fLT}^e} d\tau_{12,\,comp}$$

$$\approx \frac{1}{1-V_f + V_f S_{LT}^{-1}} d\tau_{12,\,comp} \qquad (46)$$

$$d\tau_{12,\,comp} \approx \left(1-V_f + V_f S_{LT}^{-1}\right) d\tau_m \qquad (47)$$

Then considering the integration until the time when the significant degradation of tangent modulus occurs:

$$\tau_{12} \approx \left(1-V_f + V_f S_{LT}^{-1}\right) \tau_{mY} \qquad (48)$$

where τ_{12} is applied shear stress to composite materials and τ_{mY} is yield stress of matrix. Generally the fibers have a slight misalignment, and this misalignment affects the local stress distribution of the material.

Considering the equilibrium condition of applied stress in between misalignment coordinate system and coordinate system associated with global fiber direction:

$$\sigma_{xx}\phi + \tau_{xy} = \tau_{12} \tag{49}$$

$$\sigma_{cr} = \frac{\tau_{12} - \tau_{xy}}{\phi} \approx \frac{\left(1 - V_f + V_f S_{LT}^{-1}\right)\tau_{mY} - \tau_{xy}}{\phi} \tag{50}$$

where σ_{xx} and τ_{xy} are stress in longitudinal direction and shear stress in the coordinate system associated with global fiber direction, respectively and ϕ is the misalignment angle of fiber. From this equation, the relationship of compressive strength with matrix yield stress, applied shear stress, and fiber volume fraction are represented as the linear relation, and the relationship with misalignment of fiber is represented as inversely proportional. In addition, the dependency of compressive strength for the fiber volume fraction V_f is related with the shear component of Eshelby tensor S_{LT}. When fibers are plates, $S_{LT} = 1$ and

$$\sigma_{cr} = \frac{\tau_{mY} - \tau_{xy}}{\phi} \tag{51}$$

When fibers are cylinder solids, $S_{LT} = 1/2$ and

$$\sigma_{cr} = \frac{\left(1 + V_f\right)\tau_{mY} - \tau_{xy}}{\phi} \tag{52}$$

Numerical Analysis of Material Strength using Arbitrariness Condition

Here the numerical analysis is conducted for the actual material property using the condition in Eq. (30). As the material, carbon fiber/ epoxy resin AS4/3501-6 [5] is assumed. For stress-strain curve of matrix, two kinds of curves M and N shown in Fig. 4 are applied and the results are compared. Fig. 5 (a) shows the analysis results for relationship between compressive strength and the multi-axial stresses. The shear stress reduces the compressive strength and this relation is approximately represented as the linear relation. Tensile and high compressive transverse stress also reduce the compressive strength, while under the small compressive transverse stress, the compressive strength is almost constant. In addition, the dependency of the multi-axial stresses changes with the change of the stress-strain curve of matrix. Fig. 5 (b) shows the analysis results for the relationship between compressive strength and the constituent material property. The matrix yield stress and fiber volume fraction increase the compressive strength and these relations are also close to the linear relation. The initial fiber misalignment reduces the compressive strength and this relation is close to the inversely proportional relation. The dependency of the material strength for each parameter almost agrees with the experimental results shown in the previous investigations [2–3].

CONCLUSION

Mathematical model expressing longitudinal compressive failure is obtained. There exists a state where the arbitrariness appears in the solution of equations expressing the deformation of composite materials, and the condition for onset of the arbitrariness is closely related with the initiation of the longitudinal compressive failure in the material.

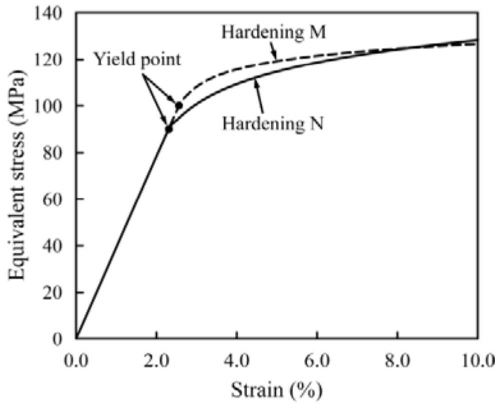

Fig. 4: Stress-strain Curves of Matrix

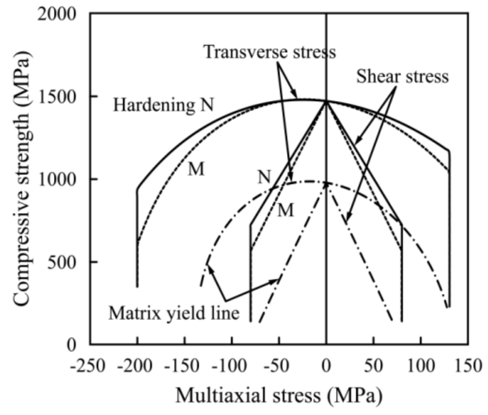

(a) Relationship with Multi-axial Stresses

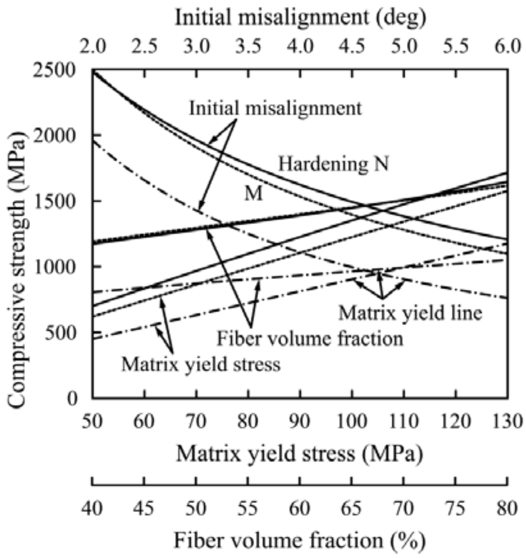

(b) Relationship with Constituent Material Property

Fig. 5: Numerical Results for Compressive Strength

REFERENCES

[1] M. J. Hinton and P. D. Soden, 'Predicting failure in composite laminates: the background to the exercise', Composites Science and Technology, 1998, Vol. 58, pp 1001-1010.

[2] C. R. Schultheisz and A. M. Waas, 'Compressive failure of composites, Part I: Testing and micromechanical theories', Progress in Aerospace Sciences, 1996, Vol. 32, pp 1-42.

[3] A. M. Waas and C. R. Schultheisz, 'Compressive failure of composites, Part II: Experimental studies', Progress in Aerospace Sciences, 1996, Vol. 32, pp 43-78.

[4] C. S. Yerramalli and A. M. Waas, 'A failure criterion for fiber reinforced polymer composites under combined compression-torsion loading', International Journal of Solids and Structures, 2003, Vol. 40, pp 1139-1164.

[5] P. D. Soden, M. J. Hinton and A. S. Kaddour, 'Lamina properties, lay-up configurations and loading conditions for a range of fibre-reinforced composite laminates', Composites Science and Technology, 1998, Vol. 58, pp 1011-1022.

[6] K. Tohgo, Y. Sugiyama and K. Kawahara, 'Ply-cracking damage and nonlinear deformation of CFRP cross-ply laminate', JSME International Journal, Series A, 2002, Vol. 45, pp 545-552.

[7] B. Budiansky, 'Micromechanics', Computers & Structures, 1983, Vol. 16, pp3-12.